Annals of Operations Research 98, 235–253, 2000

Beamforming and Interference Cancellation for Capacity Gain in Mobile Networks

SVEN NORDHOLM
ATRI, Curtin University of Technology, Perth, WA 6001, Australia

JÖRGEN NORDBERG, INGVAR CLAESSON and SVEN NORDEBO
University of Karlskrona/Ronneby, SE-372 25 Ronneby, Sweden

Abstract. The growth of wireless communication continues. There is a demand for more user capacity from new subscribers and new services such as wireless internet. In order to meet these expectations new and improved technology must be developed. A way to increase the capacity of an existing mobile radio network is to exploit the spatial domain in an efficient way. An antenna array adds spatial domain selectivity in order to improve the Carrier-to-Interference ratio (C/I) as well as Signal-to-Noise Ratio (SNR). An adaptive antenna array can further improve the Carrier-to-Interference ratio (C/I) by suppressing interfering signals and steer a beam towards the user. The suggested scheme is a combination of a beamformer and an interference canceller.

The proposed structure is a circular array consisting of K omni-directional elements and combines fixed beamforming with interference cancelling. The fixed beamformers use a weight matrix to form multiple beams. The interference cancelling stage suppresses undesired signals, leaking into the desired beam.

The desired signal is filtered out by the fixed beamforming structure. Due to the side-lobes, interfering signals will also be present in this beam. Two alternative strategies were chosen to cancel these interferers; use the other beamformer outputs as inputs to an adaptive interference canceller; or regenerate the outputs from the other beamformer outputs and generate clean signals which are used as inputs to adaptive interference cancellers.

Resulting beamformer patterns as well as interference cancellation simulation results are presented. Two different methods have been used to design the beamformer weights, Least Square (LS) and minimax optimisation. In the minimax optimisation a semi-infinite linear programming approach was used. Although the optimisation plays an essential role in the performance of the beamformer, this paper is focused on the application rather then the optimisation methods.

Keywords: spatial interference cancellation, beamforming, semi-infinite simplex algorithm

1. Introduction

The mobile radio networks are hosting more and more services. From being a provider of mainly speech communication, new services are implemented and proposed. This gives rise to a demand for more capacity. The earlier systems were mainly realtime communication where physical channels were allocated to the user. New internet services as well as machine to machine communication require high bandwidth, but mostly over shorter time frames. These new services in Personal Communication Services (PCS) create a

high demand for new modulation schemes as well as new access methods. One can see further development of GSM into schemes like EDGE and also further development of CDMA 2000(IS 95), narrow band Code Division Multiple Access and an extension to Wide band Code Division Multiple Access (WCDMA). CDMA has the potential to yield higher capacity per used resource as compared to Frequency Division Multiple Access (FDMA), or Time Division Multiple Access (TDMA). There is also considerable interest in using Space Division Multiple Access (SDMA). The method studied in this paper is a combination of Digital Beam-Forming (DBF) and adaptive Interference Cancellation(IC). The capacity gain which is apparent when using an array of antenna elements at the base station has prompted intensive research into new DBF methods [1,4,5,7,11].

The organization of this paper is as follows. A presentation of two different IC schemes are made in section 2. The demands and assumptions that have been made concerning the signal/channel model and modulation scheme will be presented in section 3. Different adaptive control algorithms for the IC scheme are evaluated in section 4. Section 5 outlines two different beamformer weight design methods. Some examples of such optimization are presented in section 6. In section 7, the two IC schemes are evaluated, and their performances are compared in terms of achieved Signal to Noise and Interference Ratio (SNIR). Finally, section 8 concludes the paper.

2. The Spatial Filtering Generalised Side-lobe Canceller

The suggested IC scheme using a Spatial Filtering-Generalised Side-lobe Canceller (SF-GSC) structure, is presented in figure 1. It consists of a beamforming part that provides fixed beams. One beam is selected to be the desired one, i.e., it contains the signal of interest (the desired signal). Signals from other directions, jammers/interferers, will also leak into the desired beam due to the side-lobes of the beam and possible multi-path. These interfering signals are also picked up by the other beams: and the output formed is employed by the IC. The IC part consists of an ordinary complex-weight noise canceller. This implies that the interfering signals can, due to their spatial diversity, be removed from the desired signal even when they cover the same frequency band, as long as they are not correlated with the desired signal. The digital modulation scheme must be selected in such a way that the different sources are not correlated.

A portion of the desired signal will also be present in the beams corresponding to the interfering signals, and will thus enter the IC filters. To solve this problem a signal regenerator is introduced between the output from the beamformers and the input to the IC filters. The SF-GSC interference canceller using a signal regenerator (SF-GSC-SR) is presented in figure 2. By using the signal regeneration circuit, the signals $(\chi_1(n), \ldots, \chi_{K-1}(n))$ are decoded and regenerated to their "original" sequence again, i.e., the dominating signal. Thus, the new inputs to the IC filters are signals which contain neither noise nor desired signal apart from some portion of erroneous decisions.

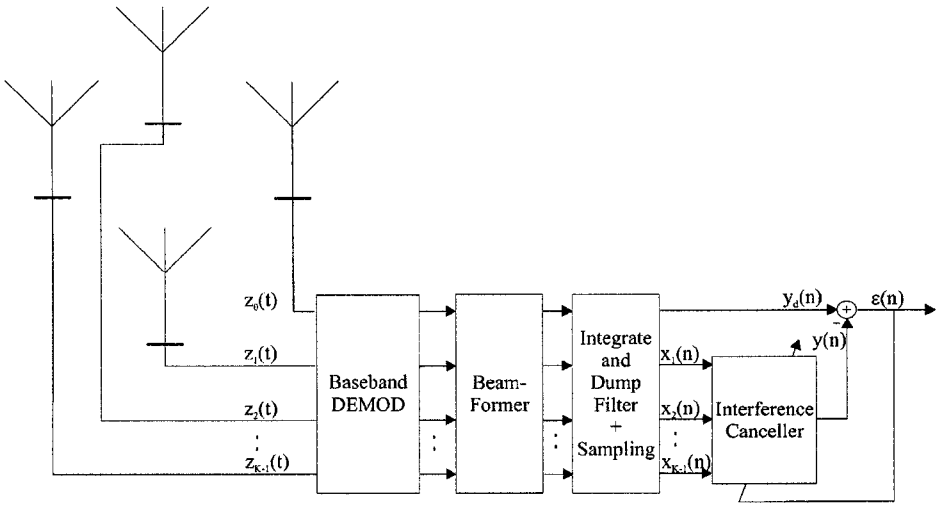

Figure 1. The SF-GSC IC filter.

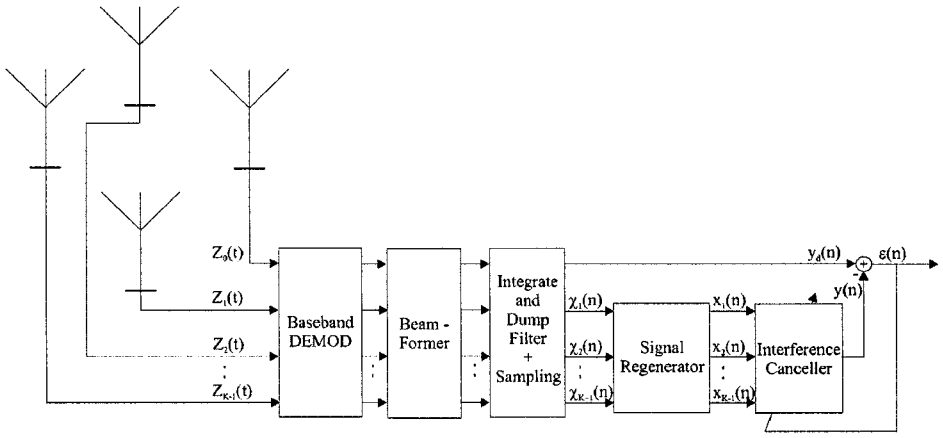

Figure 2. The SF-GSC-SR IC filter with a signal regenerating scheme.

By doing this signal regeneration there is a built-in robustness towards multi-path of the desired signal into the other beams, at least as long as there is strong incoming signal.

3. Signal and channel model

In this section a simple but yet useful signal and channel model is stated. Possible extensions of the channel model is also suggested. Finally, a derivation of the optimum LS IC filter solution is given.

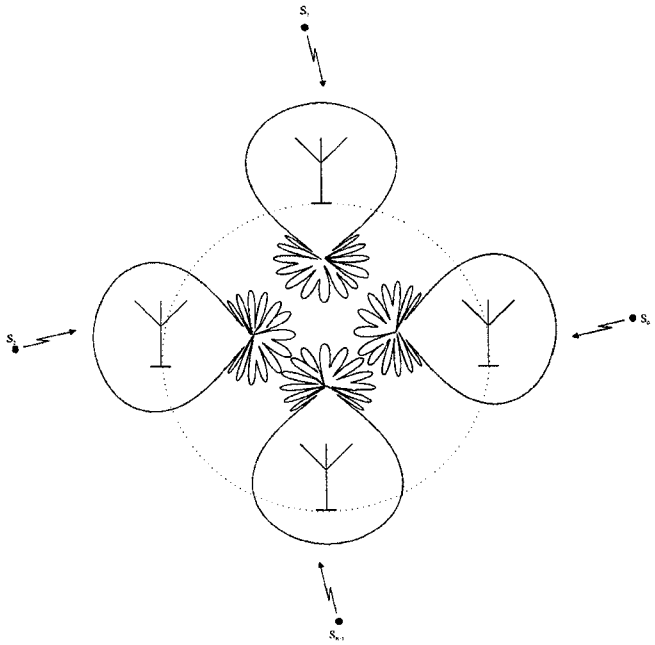

Figure 3. Assumed signal-traffic model.

3.1. *Signal model*

The signals from the transmitters are modulated around a carrier frequency f_0. The signals at each antenna element are demodulated to I and Q parts see figure 4, and sampled at the symbol rate T after the beamformer.

In order to achieve a compact formulation, a baseband equivalent notation has been used. The information signal $s_k(t)$ is assumed to be narrow-band as compared to the carrier frequency f_0. The target signal

$$s_0(t) = \sum_{n=-\infty}^{\infty} I_{0,n} h(t \quad nT) \tag{1}$$

and the jammers

$$s_k(t) = \sum_{n=-\infty}^{\infty} I_{k,n} h(t \quad nT) \tag{2}$$

are assumed to be complex baseband signals where $I_{k,n}$ represents the discrete information-bearing sequence. They are generated by K different sources with the same pulse shape $h(t) = h_I(t) + jh_Q(t)$.

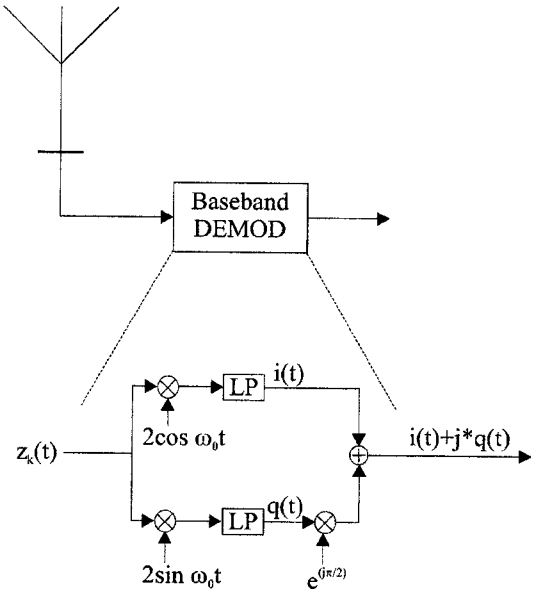

Figure 4. Conversion from bandpass signal to the baseband equivalent.

3.2. *Choice of modulation scheme*

The signal representation is chosen such that

$$E[s_k(t)s_l(t)] = 0, \quad \text{when } k \neq l,$$

where $E[\cdot]$ denotes the expected value, i.e., the signals are not correlated. This can be achieved by a modulation scheme which has a zero-symmetric signal constellation. When the modulation scheme has a non-zero symmetric signal constellation, the IC filter, might cancel the target signal. We have chosen a Quadrature Phase Shift Keying (QPSK) [15] modulation scheme.

3.3. *Channel model*

The signals are assumed to arrive as plane waves travelling with a velocity c from an angle θ_k as specified in figure 5.

Each element is disturbed by Additive White Gaussian Noise (AWGN) which is independent between the elements and has a constant spectral density $S_n(f) = \sigma_n^2$. The target signal, the jammers, and the noise are all assumed to be mutually uncorrelated. For a general array structure, the array response vector $\mathbf{d}(f_0, \theta)$ from a point source is determined by the transmitting frequency $\omega_0 = 2\pi f_0$, the wave propagation velocity c, and the orthogonal distance from the source wavefront, coming in at an angle θ, to the lth array element is denoted $\Delta_l(\theta)$. The response vector is given by

$$\mathbf{d}(f_0, \theta) = \left(e^{j\omega_0 \Delta_0(\theta)/c} \ \ldots \ e^{j\omega_0 \Delta_{K-1}(\theta)/c} \right)^{\mathrm{T}}, \tag{3}$$

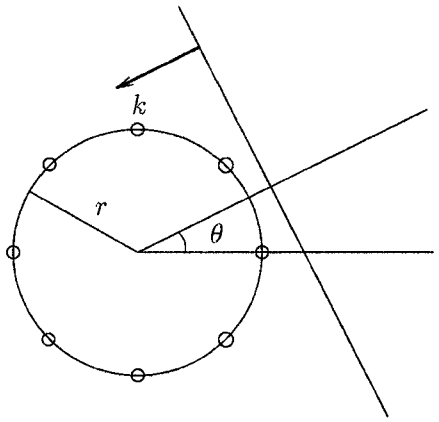

Figure 5. A planar circular array for the far-field.

where $(\cdot)^{\mathrm{T}}$ denotes the transpose operator. In equation (3) the following assumptions have been made: a reflectionless and homogeneous medium, and the signals are received with equal energy level.

This model should be extended to include multi-path and fading for real mobile communication situations, although this involved situation is not discussed here.

3.4. *Derivation of the optimal solution*

The output signal from the desired beam, $y_d(t, \theta)$, is given by

$$y_d(t, \theta) = \sum_{k=0}^{K\ 1} s_k(t)\mathbf{g}_0^H \mathbf{d}(f_0, \theta_k) + \mathbf{g}_0^H \mathbf{n}(t) = \mathbf{G}_0^H \mathbf{s}(t) + \mathbf{g}_0^H \mathbf{n}(t), \tag{4}$$

where θ is a vector containing the different angles of the impinging signals, $\mathbf{g}_0$ contains the weights of the desired beam, $(\cdot)^H$ denotes the transpose and complex conjugate operation, and $\mathbf{G}_0$ is a vector containing the total transfer functions from the source signal to the desired output, $y_d(t, \theta)$. In this expression, it has been assumed that the signals $s_k(t)$ are narrow-band compared to the carrier frequency f_0. The input correlation matrix

$$\mathbf{R}(\tau + t, t) = E\big[\mathbf{s}(t + \tau)\mathbf{s}^H(t)\big]$$

is diagonal when the target and jammer signals are mutually uncorrelated. It will, however, be cyclostationary, i.e.,

$$\mathbf{R}(\tau + t, t) = \mathbf{R}(\tau + t + T, t + T).$$

This periodicity can be avoided by taking the average over one period. The desired output autocorrelation function is expressed as

$$R_{y_d}(t + \tau, t, \theta) = \mathbf{G}_0^H E\big[\mathbf{s}(t + \tau)\mathbf{s}^H(t)\big]\mathbf{G}_0 + \mathbf{g}_0^H E\big[\mathbf{n}(t + \tau)\mathbf{n}^H(t)\big]\mathbf{g}_0. \tag{5}$$

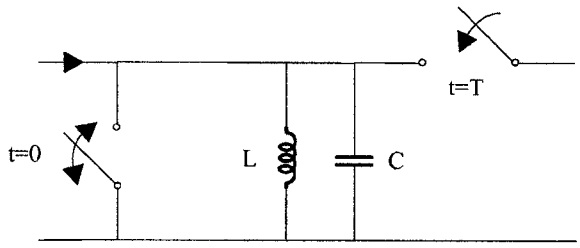

Figure 6. An integrate and dump circuit.

The input signals $x_m(t, \theta)$ to the canceller filters $h_m(t, \theta)$ are given by

$$x_m(t, \theta) = \sum_{k=0}^{K \quad 1} s_k(t)\mathbf{g}_m^H \mathbf{d}(f_0, \theta_k) + \mathbf{g}_m^H \mathbf{n}_l(t), \tag{6}$$

where $m \in [1, K \quad 1]$.

The I and Q channels, can for instance be sampled by using *Integration and Dump filters* see figure 6, which will work as matched filters under the assumption that the receiver and the transmitter are synchronised [8]. The parallel switch closes briefly at $t = 0$; this ensures that all the residual energy ($t < 0$) in the circuit does not contribute to the output at time T. The series switch is then closed briefly at $t = T$, thereby sampling the filter output at the right time.

This means that the signals $y_d[n, \theta] = y_d(t, \theta)|_{t=nT_s}$ and $x_m[n, \theta] = x_m(t, \theta)|_{t=nT_s}$ are sampled at the symbol rate $T_s = T$. The signals $y_d[n, \theta]$ and $x_m[n, \theta]$, $y_d[n]$ and $x_m[n]$ for short, are then used to adjust the weights in the IC filter. The optimal weights are found by minimizing

$$E\left[\left|\varepsilon[n]\right|^2\right] = E\left[\left|y_d[n] \quad \mathbf{w}^H \mathbf{x}[n]\right|^2\right] \tag{7}$$

with respect to the weights $\mathbf{w}$, where the received signal vector $\mathbf{x}[n]$ is defined as

$$\mathbf{x}[n] = \left[x_1[n]\, x_2[n] \ \ldots \ x_{K \quad 1}[n]\right]^{\mathrm{T}}.$$

The optimal solution is arrived at by solving the following linear equation system:

$$\mathbf{R}_{\mathbf{xx}}\mathbf{w} = \mathbf{P}_{\mathbf{x}y_d}, \tag{8}$$

where $\mathbf{R}_{\mathbf{xx}} = E(\mathbf{x}[n]\mathbf{x}^H[n])$ and $\mathbf{P}_{\mathbf{x}y_d} = E(\mathbf{x}[n]y_d^H[n])$.

4. The adaptive IC filter

The SF-GSC and the SF-GSC-SR scheme have different demands on the adaptive control algorithm that controls the adaptive IC filter, see figure 7.

In the SF-GSC case, the adaptive control algorithm must compensate for the fact that the target signals leak into the other beams. This compensation is not necessary in the SF-GSC-SR situation due to the inclusion of the signal regeneration scheme, see

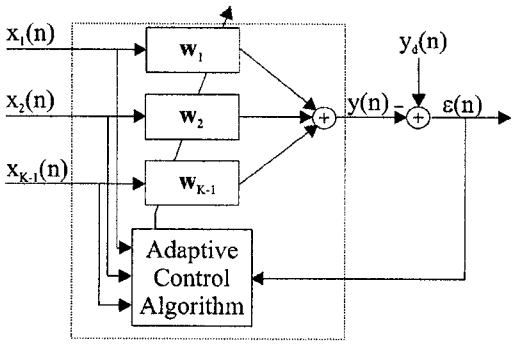

Figure 7. An adaptive interference cancelling structure.

figure 2. The performance of the IC filter depends upon the sidelobes of the beams. If the beams can be designed with a narrow main-lobe and high side-lobe suppression, the canceller will operate better. The array configuration used in this study is a circular configuration. When the array consists of many antenna elements a narrow main-lobe can be obtained.

4.1. SF-GSC-SR

The algorithm used for cancelling the interference in the SF-GSC-SR case is the Normalized Least Mean Squares (LMS) algorithm. In figure 7 the adaptive IC filter is presented.

Define $\mathbf{x}[k]$ and $\mathbf{w}[k]$ as a concatenated received signal vector and weight vector, respectively. Then, at time $t = nT_s$ $(n = 1, 2, \ldots)$, where T_s is the sampling period, $\mathbf{x}[n]$ and $\mathbf{w}[n]$ can be written as

$$\begin{aligned}\mathbf{x}[n] &= \left[x_1[n]x_1[n \quad 1] \ldots x_1[n \quad L+1] \ldots x_{K\ 1}[n] \ldots x_{K\ 1}[n \quad L+1]\right]^{\mathrm{T}},\\ \mathbf{w}[n] &= \left[w_{11}[n]w_{12}[n] \ldots w_{1L}[n] \ldots w_{(K\ 1)1}[n]w_{(K\ 1)2}[n] \ldots w_{(K\ 1)L}[n]\right]^{\mathrm{T}},\end{aligned} \tag{9}$$

where L denotes the filter length of each filter. For complex signals, both $\mathbf{x}[n]$ and $\mathbf{w}[n]$ are represented by a complex vector. The output signal of the LMS spatial equaliser $y[n]$ is given by

$$y[n] = \mathbf{w}^H[n]\mathbf{x}[n]. \tag{10}$$

The weight update equation is defined by

$$\mathbf{w}[n+1] = \mathbf{w}[n] + \frac{\alpha(y_d[n] \quad y[n])^*\mathbf{x}[n]}{\mathbf{x}^H[n]\mathbf{x}[n]}, \tag{11}$$

where $(\cdot)^*$ denotes the complex conjugate operator and α is the stepsize, that controls the adaptive behaviour of the IC filters [9].

4.2. *SF-GSC*

Since the target signal leaks into the other beams, a method to prevent target cancellation is needed. One way to accomplish this is to use the Leaky-NLMS [13], L-NLMS, as the adaptive control algorithm in the SF-GSC scheme. Using the same definitions as in the NLMS algorithm, the weight update equation is now defined by

$$\mathbf{w}[n+1] = \mathbf{w}[n]\gamma + \frac{\alpha(y_d[n] \quad y[n])^*\mathbf{x}[n]}{\mathbf{x}^H[n]\mathbf{x}[n]}, \tag{12}$$

where γ is a leakage factor. Using a leaky algorithm is equivalent for the algorithm to inject AWGN at the adaptive filter inputs when updating the weights, although there is no noise present disturbing the output. The strength of the equivalent white noise is given by [13]

$$\sigma_n^2 = \frac{1 \quad \gamma}{2} \tag{13}$$

which, when appropriately chosen, dominates over the side-lobe leakage of the target signal. Due to the leaky-noise the achievable Signal-to-Noise-Interference Ratio, SNIR value will be reduced but it will prevent the target signal from being cancelled.

5. Beamformer design

The planar circular array is defined by K sensor elements evenly distributed on a circle, and an incident wave front propagating in the same plane as the array, see figure 5. We consider the far-field and narrow-band case where the phase of the wave front is given by $e^{j(2\pi f_0 t \quad \mathbf{k}^T\mathbf{r})}$, where f_0 is the carrier frequency, t is the time, $\mathbf{k} = \frac{2\pi f_0}{c}(\cos\theta, \sin\theta)$ is the wave vector, c is the speed of propagation, θ is the angle of incidence, and $\mathbf{r}$ is the evaluated spatial point. The array elements have the spatial positions $\mathbf{r}_k = r(\cos(k\frac{2\pi}{K}), \sin(k\frac{2\pi}{K}))$, where $k = 0, \ldots, K \quad 1$ and r is the radius of the array circle.

With the phase centre at the origin (centre) of the array, the array angular transfer function is given by

$$G(\theta) = \sum_{k=0}^{K \quad 1} g_k a_k(\theta) e^{j2\pi f_0(r/c)\cos(k2\pi/K \quad \theta)}, \tag{14}$$

where g_k are the complex array weights, and $a_k(\theta)$ are the responses of the individual sensors. In order to simplify subsequent discussion but still preserve generality, we will assume that $a_k(\theta) = 1$.

5.1. *Least square solution*

One way to design a circular beamformer is to use a least squares design where the design objective is to minimize the Euclidean norm

$$\left\| \mathbf{G}_d \quad \mathbf{g}_c^H \mathbf{D}_c \right\|_2 \tag{15}$$

with respect to the complex vector $\mathbf{g}_c$, where $\mathbf{g}_c$ is a K long beamformer weight vector. Here, $\mathbf{D}_c$ is an $K \times I$ matrix where $\mathbf{D}_c = [\mathbf{d}_c(f_0, \theta_1) \cdots \mathbf{d}_c(f_0, \theta_I)]$ and $\mathbf{G}_d$ is an $I \times 1$ vector where $\mathbf{G}_d = [G_d(\theta_1) \cdots G_d(\theta_I)]^{\mathrm{T}}$ defined over I angular samples $\theta_1, \ldots, \theta_I$ at one frequency f_0. As a design example, we will consider the desired response

$$G_d(\theta) = \begin{cases} 1, & \theta_p \leqslant \theta \leqslant \theta_p, \\ 0, & \theta_s \leqslant \theta \leqslant 2\pi \quad \theta_s, \end{cases} \tag{16}$$

where the positive angles θ_p and θ_s define the "pass-band" and "stop-band" edges.

5.2. *Minimax solution*

It is also possible to use a minimax approach to design a circular beamformer. In this case it is ideal to use the infinite–dimensional complex approximation formulation, equations (17)–(19) and (21), which is amenable to a solution using the extended simplex algorithm [2].

The complex specification may be given in the form

$$\left| G_d(\theta) \quad \mathbf{g}_c^H \mathbf{d}_c(f_0, \theta) \right| \leqslant e(\theta), \quad \theta \in \Omega, \tag{17}$$

where $G_d(\theta)$ is the desired complex response, $e(\theta)$ is a prescribed (strictly positive) upper bound and Ω is the angular domain. The frequency dependency is omitted in the sequel. It is assumed that $G_d(\theta)$ is a continuous function. This narrow-band case with complex weights, $\mathbf{g}_c = \mathbf{g}_R + j\mathbf{g}_I$, can be reformulated by defining $G(\theta) = \mathbf{g}_c^H \mathbf{d}_c(\theta) = \mathbf{g}^{\mathrm{T}} \mathbf{d}(\theta)$, where $\mathbf{g}^{\mathrm{T}} = [\mathbf{g}_R^{\mathrm{T}} \;\; \mathbf{g}_I^{\mathrm{T}}]$ and $\mathbf{d}^{\mathrm{T}}(\theta) = [\mathbf{d}_c^{\mathrm{T}}(\theta) \;\; j\mathbf{d}_c^{\mathrm{T}}(\theta)]$. In this case, the number of real array coefficients is $2K$.

The circular array is an example of a situation when a complex response must be considered. It is not feasible to obtain a real- or linear-phase response by employing coefficient symmetry as with an equi-spaced linear array, since the spatial sampling with the circular array is non-uniform.

We now pose the following design criterion

$$\min_{\mathbf{g} \in R^N} \max_{\theta \in \Omega} v(\theta) \left| G_d(\theta) \quad \mathbf{g}^{\mathrm{T}} \mathbf{d}(\theta) \right| \tag{18}$$

$$\text{subject to} \quad \mathbf{P}\mathbf{g} \leqslant \mathbf{p}, \tag{19}$$

where $v(\theta)$ is a strictly positive weighting function, $\mathbf{P}$ is a $K \times 2K$ constraint matrix, and $\mathbf{p}$ is a $K \times 1$ constraint vector. Note that with the choice of weighting $v(\theta) = 1/\varepsilon(\theta)$, the specification in equation (17) will be satisfied if and only if the optimum objective value in equation (18) is less than or equal to one.

According to the *real rotation theorem* [3], a magnitude inequality in the complex plane can be expressed in the following equivalent form:

$$|z| \leqslant \delta \Leftrightarrow \Re\{z e^{j\phi}\} \leqslant \delta \quad \forall \phi \in [0, 2\pi], \tag{20}$$

where z is a complex number, δ is a real and positive number, and $\Re\{\cdot\}$ denotes the real part.

By making use of equation (20), the nonlinear approximation problem in equations (18)–(19) can be reformulated as the following continuous semi-infinite linear program:

$$\begin{cases} \min \delta \\ v(\theta)\Re\{(G_d(\theta) \quad G(\theta)) \cdot e^{j\phi}\} \leqslant \delta, \\ \mathbf{Pg} \leqslant \mathbf{p}, \end{cases} \tag{21}$$

where δ is an additional real variable, $\theta \in \Omega$ and $\phi \in [0, 2\pi]$.

The linear program in equation (21) is called (continuous) semi-infinite since the constraint set is infinite (uncountable) and the number of variables is finite.

Define the $(2K + 1) \times 1$ vectors $\mathbf{y}$ (variable) and $\mathbf{b}$ (constant) by

$$\mathbf{y} = \begin{pmatrix} \mathbf{g} \\ \delta \end{pmatrix}, \qquad \mathbf{b} = \begin{pmatrix} \mathbf{0} \\ 1 \end{pmatrix}, \tag{22}$$

where $\mathbf{0}$ is an $2K \times 1$ vector of zeros. Further, let the $2K \times 1$ vector function $\mathbf{a}(\theta, \phi)$ and the scalar function $c(\theta, \phi)$ be defined by

$$\mathbf{a}(\theta, \phi) = v(\theta)\Re\{\mathbf{d}(\theta) \cdot e^{j\phi}\}, \tag{23}$$

$$c(\theta, \phi) = v(\theta)\Re\{G_d(\theta) \cdot e^{j\phi}\}. \tag{24}$$

The linear program equation (21) is now restated in the following form

$$\begin{cases} \min \mathbf{b}^{\mathrm{T}}\mathbf{y} \\ \begin{bmatrix} \mathbf{a}^{\mathrm{T}}(\theta, \phi) & 1 \\ \mathbf{P} & \mathbf{0} \end{bmatrix} \mathbf{y} \geqslant \begin{bmatrix} c(\theta, \phi) \\ \mathbf{p} \end{bmatrix}, \end{cases} \tag{25}$$

where $\mathbf{0}$ is an $K \times 1$ vector of zeros.

The design problem in equations (18) and (19) can now be solved by formulating the following (dual) continuous semi-infinite linear program

$$(\mathrm{D}) \begin{cases} \min \mathbf{b}^{\mathrm{T}}\mathbf{y} \\ \mathbf{A}_\alpha^{\mathrm{T}}\mathbf{y} \geqslant c_\alpha, \end{cases} \tag{26}$$

where $\mathbf{A}_\alpha^{\mathrm{T}}$ and c_α are the rows of the left hand side constraint matrix and the elements of the right hand side constraint vector in equation (25), respectively. Here α is an index belonging to a closed index set $\mathcal{A} \subset R^n$, which has a one-to-one correspondence with the constraint rows of equation (25). The set $\mathcal{A}$ can be constructed as follows. Let $\alpha = (\theta, \phi, i, l)$ where $l = 1$ or 2 since there are 2 types of constraints in equation (25). If $l = 1$, then $(\theta, \phi) \in \Omega \times [0, 2\pi]$ and $i = 1$. If $l = 2$, then $\theta = \theta_0$ (fixed value), $\phi = 0$ and $i = 1, \ldots, K$. The formulation of equation (26) is now in a form which

has been investigated in, e.g., [2]. We refer to equation (26) as the dual formulation since it corresponds to the dual of a linear program in standard form [2,12]. Several solution methods exits for this optimisation problem, see, e.g., [2,6,10,14]. In this paper a standard semi-infinite simplex algorithm as described in [14] was used.

6. Beamformer design examples

In the design examples below, the following common parameters have been used: number of complex coefficients $K = 8$, desired response defined by $\theta_p = 10 \cdot \pi/180$ (10 degrees) and $\theta_s = 40 \cdot \pi/180$ (40 degrees), number of spatial samples $I = 720$.

Figure 8 shows the resulting array patterns for two different design situations with $r/\lambda = 1/2$ and where $\lambda = c/f_0$ is the wave length. The polar plots show the magnitude of the response $G(\theta)$ in dB. Here, the origin corresponds to a magnitude of 60 dB or less, and the outer circle corresponds to the 0 dB level (the plots show $\max\{0, 20\log|G(\theta)| + 60\}$).

In figure 8, the solid line shows the resulting array pattern for a least squares design according to the criterion given in equation (15). The dashed line shows the array pattern corresponding to the unconstrained min–max problem, equation (18), with constant weighting $v = 1$. These two figures illustrate typical features when comparing a least squares design to a uniform approximation. The least squares design appears to achieve better overall stop band rejection, whereas the minimax design gives the best possible

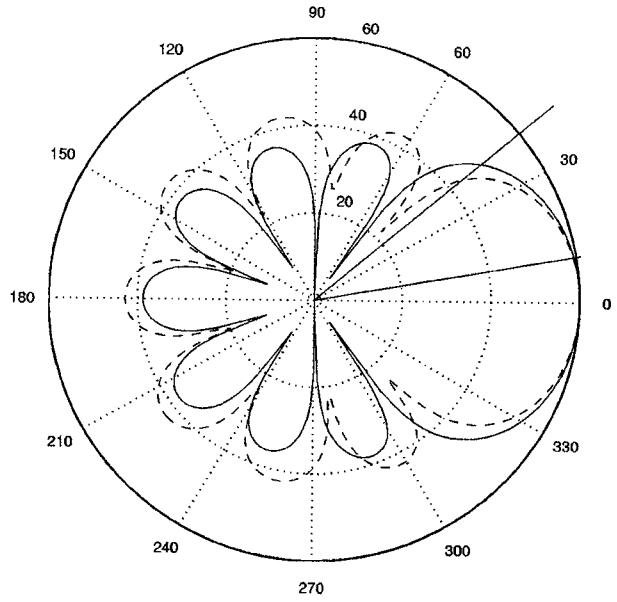

Figure 8. Array pattern given in dB, least squares solution (solid line) and minimax solution (dashed line).

rejection at the stop band edge (the pass and stop band edges are indicated by straight lines).

These comparisons are given as illustrations of possible performance. The least squares and min–max design criteria correspond to different norms, and therefore it is often futile to compare these methods strigthforwardly. However, if the design specification is given as an upper bound on the design error as in equation (17), it is practical and straightforward to employ the weighted minimax criteria to obtain a solution (if any).

The latter situation is illustrated in figure 9 which shows a non-uniformly weighted min–max design. Here, the error envelope $\varepsilon(\theta)$ is defined by

$$\varepsilon(\theta) = \begin{cases} 1 \quad 10^{\frac{3}{20}}, & 0 \leqslant \theta \leqslant \theta_p, \\ 10^{\frac{15(\pi - \theta)}{20(\pi - \theta_s)} \frac{60}{20}}, & \theta_s \leqslant \theta \leqslant \pi, \end{cases} \tag{27}$$

and $\varepsilon(\ \theta) = \varepsilon(\theta)$. The angular weighting is then given by $v(\theta) = 1/\varepsilon(\theta)$. The definition of equation (27) means that the pass band magnitude is greater than 3 dB and that the stop band magnitude is bounded by an envelope starting at 45 dB at θ_s rad, and decreasing linearly to 60 dB at π rad. The stop band envelope is included in figure 9.

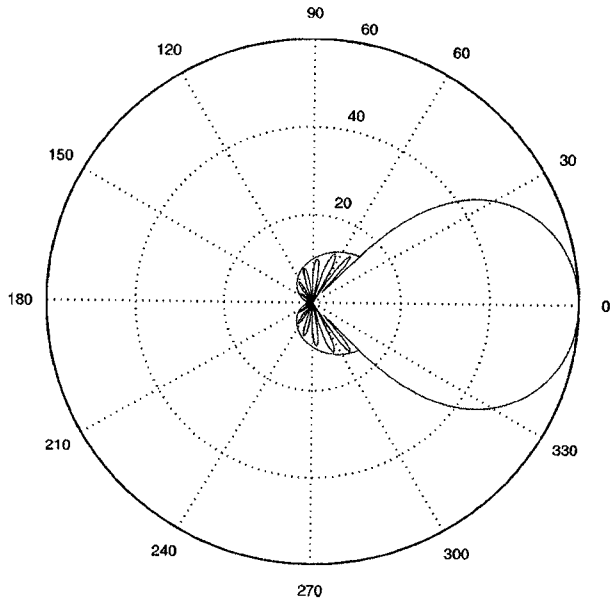

Figure 9. Array pattern in dB. Minimax solution, non-uniform weighting.

7. Interference Cancellation (IC) examples

The study covers two different situations one where a four sector antenna has been completed with a IC filter, the second is a comparison of 8 element beamformers designed using LS and minimax criterion, respectively. The first study clearly shows the benefits of the spatial multiuser detection. The second study shows how the performance depends on the properties of the fixed beamformer weights. The following assumption has been made about the traffic situation: there exists a dominant signal in each beam, see figure 3. All the simulation results in this chapter are compared to a minimum mean square solution according to equation (7). For the SF-GSC-SR this means that in some cases this solution can be out-performed since there will be essentially no noise in the input signals to the IC filters.

7.1. Four sector antenna

In the first two simulations, figures 11 and 12, a four element beamformer, as shown in figure 10, was used. It is a LS designed beamformer with a radius of $\lambda/4$ and four antenna elements. The number of beams is also 4, and they are evenly distributed, i.e., the centre is at 0, 90, 180 and 270 degrees.

Figures 11 and 12 show a performance comparison between the two suggested interference cancellation methods SF-GSC-SR and SF-GSC. From figure 11 one can see that a faster convergence will be obtained for the SF-GSC-SR scheme. Both schemes resulted in approximately the same SNIR. This was expected since the target signal arrived in the centre of the beam, i.e., no target signal leaked into the other beams thus no

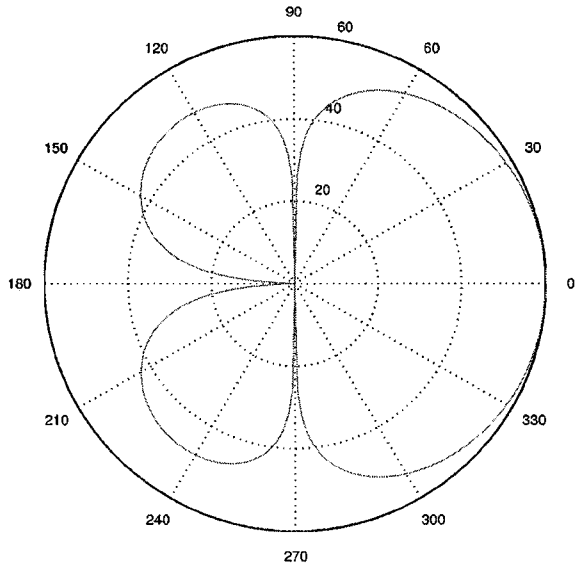

Figure 10. A LS-designed beamformer with four antenna elements.

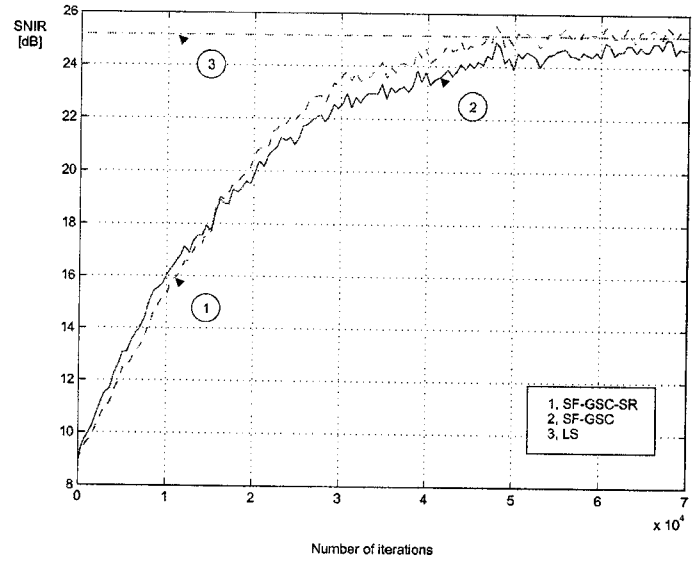

Figure 11. Convergence curves for IC vs # of iterations. Target from = 0 degrees, jammers arriving at angles [70, 190, 250]. SNR at each individual antenna element is 20 dB. Interference signals and target signal have equal power.

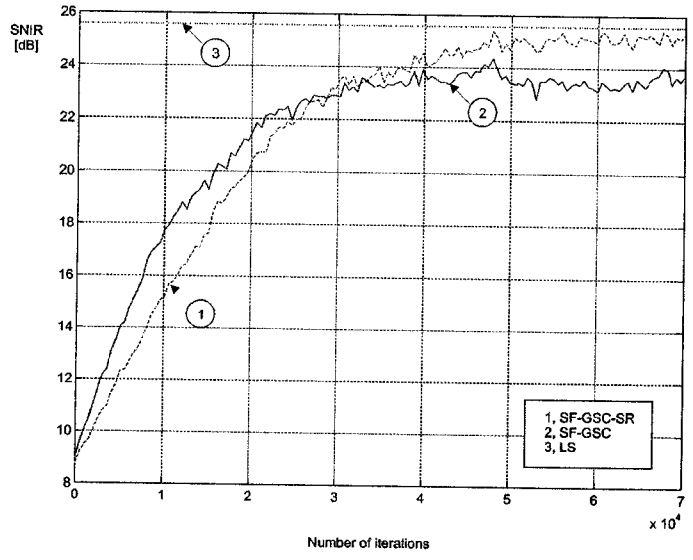

Figure 12. Convergence curves for IC vs # of iterations. Target from 10 degrees, jammers arriving at angles [70, 190, 250]. SNR at each individual antenna element is 20 dB. Interference signals and target signal have equal power.

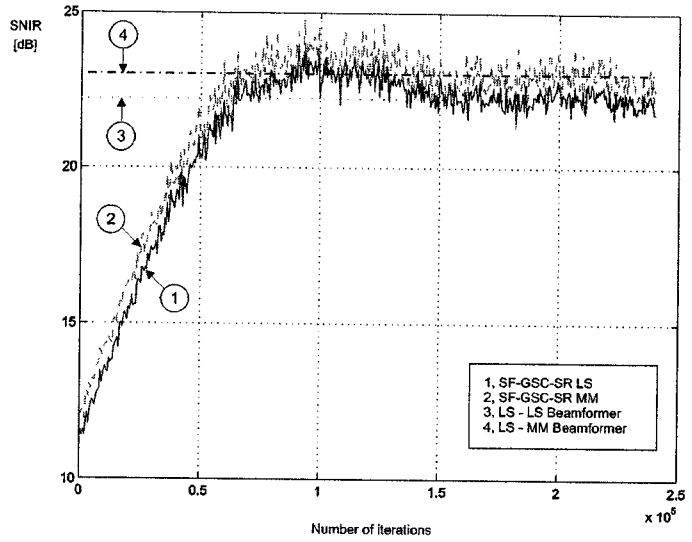

Figure 13. Convergence curves for IC vs # of iterations. Target from 0 degrees. Jammers arriving at angles [45, 100, 145, 170, 220, 280, 315]. SNR at each individual antenna element is 20 dB. Interference signals and target signal have equal power.

target cancellation could occur. In figure 12, the Angle Of Arrival (AOA) is 10 degrees and now the SF-GSC cannot reach the same SNIR value as the SF-GSC-SR algorithm due to the fact that the target signal is leaking through to the other beams. As can be seen from figure 11 the MMSE solution can be out performed due to the decoding and regeneration of the signals into the IC filters.

7.2. Comparison of LS and minimax beamformers

In this study an 8 element array has been used. The two used beamformers are presented in figure 8, the number of beams is 8. In all of the following simulations the SF-GSC-SR IC filter is used. Figures 13 and 14 show the results, when the AOA for the desired signal equals 0 and 10 degrees respectively. The solid line corresponds to the LS designed beams and the dashed line corresponds to the minimax designed beams. These are evenly distributed, i.e., the centre is at 0, 45, 90, and so on. There is one desired beam, and 7 beams for the IC filters. As can be seen in the figures, the minimax designed beamformers give slightly better performance in the given situation. This is due to the more narrow stop band edge, which is crucial in this situation since it determines how much of the desired signal leaks into the closest beams.

The results in figures 13 and 14 indicate that the IC filter will perform better when the AOA of the target signal is 10^o rather than 0^o. This is due to the fact that the sidelobes have their maximum level close to the other beam's centre. A solution to this problem is to have several point constraints that force the beamformer to have a minimum at the other beam's centre. The used design method facilitates the inclusion of point constraints

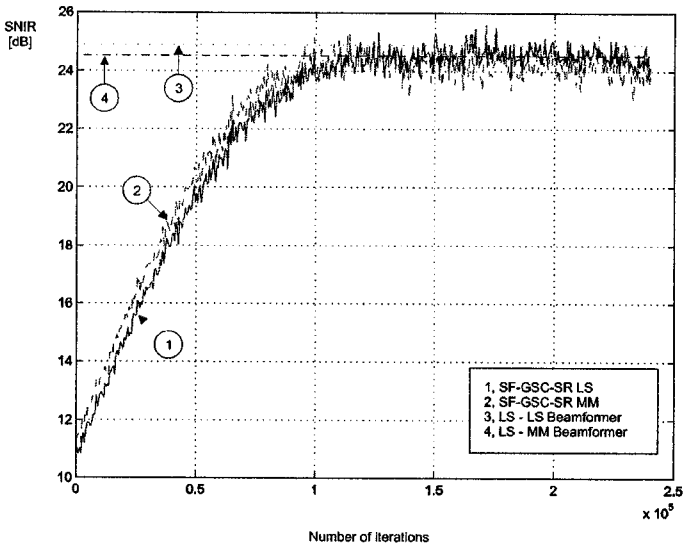

Figure 14. Convergence curves for IC vs # of iterations. Target from 10 degrees. Jammers arriving at angles [45, 100, 145, 170, 220, 280, 315]. SNR at each individual antenna element is 20 dB. Interference signals and target signal have equal power.

and the result is presented in figure 15, and the simulation results using this beamformer are presented in figure 16. The maximum SNIR value is now achieved when the AOA equals 0^o.

Due to the point constraints the beamformer has lost the equal suppress level of the sidelobes that was achieved in the min-max beamformer presented in figure 8. For certain AOA and interference situations with point-constrained beamformer the resulting SNIR will be better. However, under some other conditions it will perform worse than the beamformer in figure 8. It is also much simpler to evaluate a beamformer that has an equal min-suppression of the side-lobes, and investigate the worst case scenario of this beamformer. Still, when the AOA information is available this is a possibility.

8. Conclusions and further research

A method has been presented which shows good capability of suppressing interfering signals which are spatially separated from the target signal. The method has been further improved by including a signal regenerator in the scheme. This improvement allows a certain degree of multipath which otherwise is cumbersome to IC schemes. Methods are presented for designing beamformers for circular arrays using both a least squares criterion as well as a minimax design.

Further research needs to be done in order to quantify the size of allowable multipath and should also include some urban fading models for the propagation. In order to improve the SNIR level of the signals into the signal regenerator, some kind of pre-

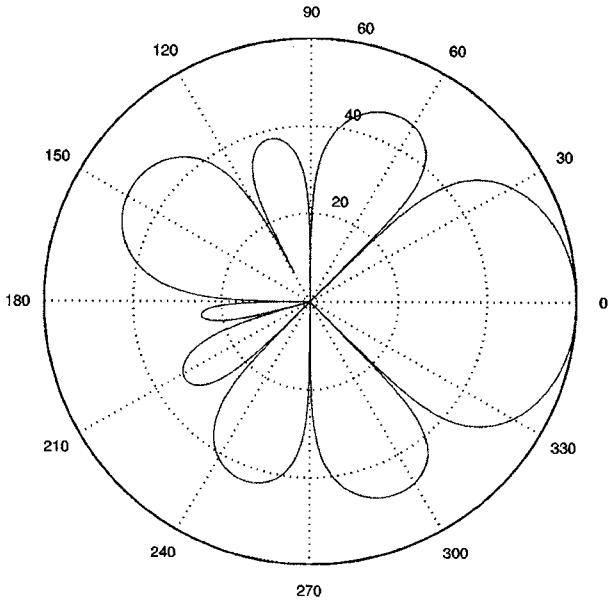

Figure 15. Min-max array design with point constraint.

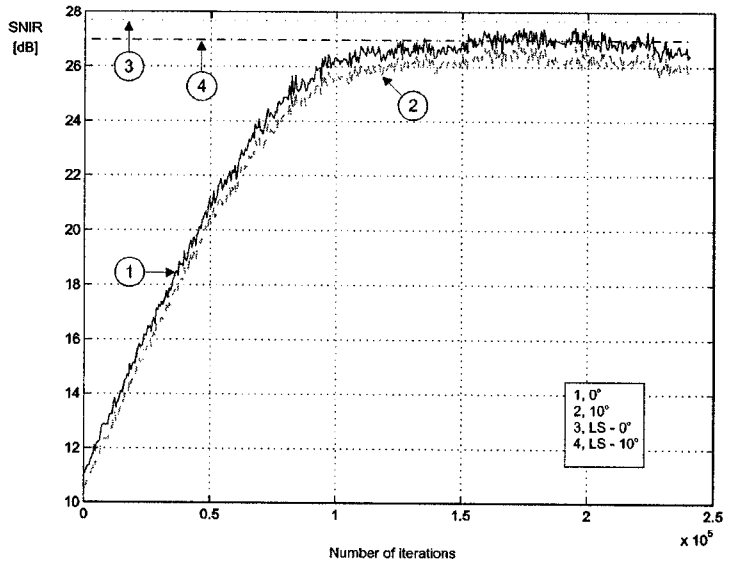

Figure 16. Convergence curves for IC vs # of iterations. Target from 0 degrees. Jammers arriving at angles [45, 100, 145, 170, 220, 280, 315]. SNR at each individual antenna element is 20 dB. Interference signals and target signal have equal power.

processing such as a decorrelator could be included; the amount of erroneous decision would be reduced and a more clear estimate of the interfering signals could be achieved. This would improve the overall performance of the IC filter. Further studies of optimum solutions are also of interest to obtain performance limits. Another issue would be to find results on the Bit-Error-Rate (BER) for the suggested scheme.

References

[1] S. Andersson, M. Millnert, M. Viberg and B. Wahlberg, An adaptive array for mobile communication systems, IEEE Transactions on Vehicular Technology 40 (1991) 230–236.
[2] E.J. Anderson and P. Nash, *Linear Programming in Infinite-Dimensional Spaces* (Wiley, New York, 1987).
[3] X. Chen and T.W. Parks, Design of FIR filters in the complex domain, IEEE Transactions on Acoustics, Speech, and Signal Processing 35(2) (1987) 144–153.
[4] I. Claesson and S. Nordholm, A spatial filtering approach to robust adaptive beamforming, IEEE Transactions on Antennas and Propagation 40(9) (1992) 1093–1096.
[5] M.H. Er and A. Cantoni, A unified approach to the design of robust narrow-band antenna array processors, IEEE Transactions on Antennas and Propagation 38(1) (1990) 17–23.
[6] M.A. Goberna and M.A. López, *Semi-Infinite Linear Optimization*, Wiley Series in Mathematical Methods in Pratice 2 (Wiley, Chichester, England, 1998).
[7] L.J. Griffiths and C.W. Jim, An alternative approach to linearly constrained adaptive array processing, IEEE Transactions on Antennas and Propagation 30(1) (1982) 27–34.
[8] S. Haykin, *Digital Communication* (Wiley, 1988).
[9] S. Haykin, *Adaptive Filter Theory* (Prentice-Hall, 1996).
[10] S. Ito, Y. Liu and K.L. Teo, A dual parameterization method for convex semi-infinite programming, in: *Optimization Techniques and Applications*, eds. L. Cacetta et al. (1998) pp. 558–565.
[11] J. Litva and T.K. Lo, *Digital Beamforming in Wireless Communications* (Artec House, 1996).
[12] D.G. Luenberger, *Linear and Nonlinear Programming* (Addison-Wesley, 1984).
[13] S. Nordebo, I. Claesson and S. Nordholm, Adaptive beamforming: spatial filter designed blocking matrix, IEEE Journal of Oceanic Engineering 19(4) (1994) 583–590.
[14] S. Nordebo and Z. Zang, Semi-infinite linear programming: A unified approach to digital filter design with time and frequency domain specifications, IEEE Transactions on Circuits and Systems-II: Analog and Digital Signal Processing 46(6) (1999) 765–775.
[15] J.G. Proakis, *Digital Communications* (McGraw-Hill, 1995).